

## Accepted Manuscript

Targeted Fluorescent Probes for Detection of Oxidative Stress in the Mitochondria

Nazmiye B. Yapici, Srinivas Mandalapu, K. Michael Gibson, Lanrong Bi

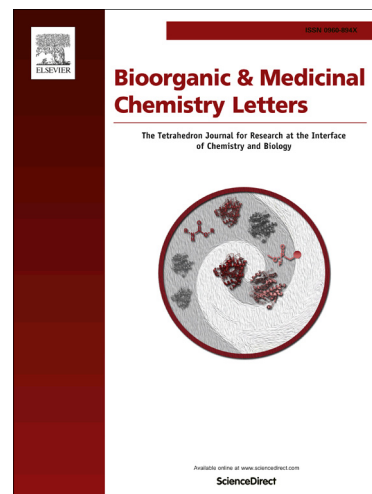
PII: S0960-894X(15)00715-5  
DOI: <http://dx.doi.org/10.1016/j.bmcl.2015.07.011>  
Reference: BMCL 22900

To appear in: *Bioorganic & Medicinal Chemistry Letters*

Received Date: 12 May 2015  
Revised Date: 30 June 2015  
Accepted Date: 2 July 2015

Please cite this article as: Yapici, N.B., Mandalapu, S., Michael Gibson, K., Bi, L., Targeted Fluorescent Probes for Detection of Oxidative Stress in the Mitochondria, *Bioorganic & Medicinal Chemistry Letters* (2015), doi: <http://dx.doi.org/10.1016/j.bmcl.2015.07.011>

This is a PDF file of an unedited manuscript that has been accepted for publication. As a service to our customers we are providing this early version of the manuscript. The manuscript will undergo copyediting, typesetting, and review of the resulting proof before it is published in its final form. Please note that during the production process errors may be discovered which could affect the content, and all legal disclaimers that apply to the journal pertain.



# Targeted Fluorescent Probes for Detection of Oxidative Stress in the Mitochondria

Nazmiye B. Yapici<sup>a</sup>, Srinivas Mandalapu<sup>a</sup>, K. Michael Gibson<sup>b</sup>, Lanrong Bi<sup>a\*</sup>

<sup>a</sup> Department of Chemistry, Michigan Technological University, Houghton, MI, USA

<sup>b</sup> Experimental & Systems Pharmacology, College of Pharmacy, Washington State University, Spokane, WA 99201

Corresponding Author: Lanrong Bi, Email: [Lanrong@mtu.edu](mailto:Lanrong@mtu.edu)

**KEYWORDS:** Mitochondria-Targeting, Oxidative Stress, Fluorescence Probes.

*Supporting Information Placeholder*

**ABSTRACT:** Mitochondrial oxidative stress has been implicated in aging, neurodegenerative diseases, diabetes, stroke, ischemia/reperfusion injury, age-related macular degeneration (AMD) and cancer. Recently, we developed two new mitochondria-targeting fluorescent probes, MitoProbes I/II, which specifically localize in mitochondria and employed both in vivo and in vitro for detection of mitochondrial oxidative stress. Here, we report the design and synthesis of these agents, as well as their utility for real-time imaging of mitochondrial oxidative stress in cells.

Mitochondrial oxidative stress is implicated in aging and neurodegeneration, diabetes, cardiovascular disease, ischemia/reperfusion injury, age-related macular degeneration (AMD) and cancer.<sup>1-11</sup> The generation of reactive oxygen species (ROS) during mitochondrial oxidative phosphorylation is a normal cellular process that can have damaging effects when uncontrolled. An often employed approach for ROS detection, electron spin resonance (ESR) spectroscopy is limited by low spatial resolution and a lack of applicability to real-time imaging of ROS at the single cell level. Conversely, fluorescent analysis is a powerful and convenient tool for monitoring the biological events in a living specimen. Unfortunately, few fluorescent probes for the detection of oxidative stress are currently available.<sup>12,13</sup> For example, fluorescent probes such as dihydorhodamine are not preferentially localized intracellularly prior to oxidation.<sup>12</sup> Typical mitochondrial dyes are limited in their utility because of instability upon illumination. Rhodamine 123, for example, is susceptible to photobleaching and exhibits strong photoinduced toxicity.<sup>14</sup> As well, the JC-1 dye is not mitochondrial specific, rendering it unsuitable for evaluation of intracellular mitochondrial function.<sup>14</sup> Recently, Chang et al developed a fluorescent probe for mitochondrial specific H<sub>2</sub>O<sub>2</sub> detection.<sup>15,26</sup> Here, we report the design and synthesis of two novel fluorescent probes that specifically target mitochondria and show convincing evidence for utility in monitoring mitochondrial oxidative stress in real time.

Design and Synthesis of Mitochondria-Targeting Fluorescent Probes (MitoProbes I/II) for Monitoring Mitochondrial Oxidative Stress. Our strategy for monitoring mitochondrial oxidative stress is to employ fluorogenic spin probes that can be detected by both fluorescence and ESR spectroscopy. The combination of both nitroxide and fluorescent

moieties in one molecule yields a non-fluorescent compound. This likely results from quenching of the excited singlet state of aromatic fluorescent compounds by the nitroxide moiety.<sup>16,17</sup> Free radicals can react efficiently with the nitroxide moiety of the probes. This results in a diamagnetic compound, thereby eliminating intra-molecular quenching and enhancing fluorescence. The fluorescent probes we designed, which contain cationic residues, can pass through the outer mitochondrial membrane. The inner membrane is much more hydrophobic, and therefore it is important to preserve a high degree of lipophilicity in our molecular design. Thus, our newly synthesized fluorescent probes (MitoProbe I/II) contain both cationic and hydrophobic residues to provide electrostatic driving forces for uptake through both mitochondrial membranes (Figure 1).

The synthesis of MitoProbe I/II was accomplished under mild conditions (Scheme S1). Starting from rhodamine B, a tertiary amide can be readily prepared by coupling with alkyne derivatized piperazine. Formation of a tertiary amide bond between rhodamine B and piperazine as a linker moiety prevents cyclization of the rhodamine derivative into a non-fluorescent lactam form. Thus, MitoProbe I/II could be readily prepared via “click reaction” via reaction of the tertiary amide with 4-azido-tempo, which was synthesized from 4-hydroxyl-2, 2, 6, 6-tetramethyl-piperidine 1-oxyl according to a previously reported procedure.<sup>17,18</sup> In order to avoid reduction of the nitroxide radical by sodium L-ascorbate to the non-paramagnetic hydroxylamine derivative during the click reaction, copper (I) iodide was employed as the copper (I) source instead of the Cu(II)SO<sub>4</sub>/sodium L-ascorbate system. An optimal reaction was achieved with the inclusion of 10 mol % Cu (I) iodide. All the <sup>1</sup>H NMR signals of the nitroxide-labeled compounds were broadened and the peaks that were associated with the Tempo residue did not appear in the <sup>1</sup>H NMR spectra. The signal intensities of the peaks obtained for the triazole moiety were also affected. Because of the paramagnetic broadening effect of the free radical, the target MitoProbes I/II were further treated with sodium L-ascorbate to give the corresponding hydroxylamines (non-radical), which was further characterized by <sup>1</sup>H NMR. All the intermediates were characterized by NMR, and the target compounds were further confirmed by MALDI-TOF MS and high-resolution mass spectrometry. In addition, MitoProbes were analyzed by EPR spectroscopy to further confirm the presence of the intact nitroxide label (Figure S1). MitoProbes I/II are stable and were stored at room temperature in sealed bottles and protected from light until use.

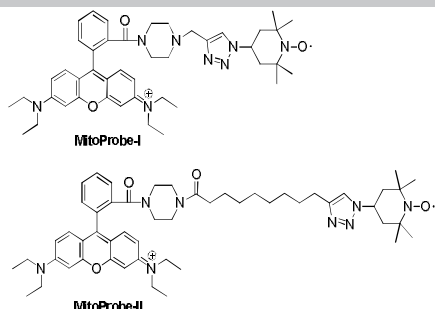


Fig. 1. Chemical structure of MitoProbes I/II.

**Intracellular Localization of MitoProbe I/II.** Compared to non-neoplastic cells, oxidative stress is significantly enhanced in tumor cells. Multiple human tumor cell lines have been reported to produce large amounts of ROS.<sup>16</sup> ROS generation by tumor cells may enhance other properties of malignancy, including tissue invasion.<sup>16</sup> To analyze the exact intracellular localization of MitoProbe I/II, counter staining with a mitochondria-specific fluorescent marker MitoTracker (Life Technologies) was performed in living HeLa (human cervical cancer) cells. HeLa cells were treated with MitoProbe I/II for 45 min, followed by washing with DPBS buffer. HeLa cells were then stained with MitoTracker FM, and subjected to confocal fluorescence microscopy. A high proportion of overlay between MitoProbe I/II and MitoTracker was clearly visible, indicating a good co-localization (Fig. 2). The presence of MitoProbe I/II appeared punctately localized within mitochondria, likely due to the presence of the membrane-permeable and cationic rhodamine moiety, which reflects the enhanced negative membrane potential across the inner mitochondrial membrane.

**Detection of Mitochondrial Oxidative Stress in Human Retinal Pigment Epithelial (ARPE) Cells Under Conditions of Stress.** The retina is particularly susceptible to oxidative stress because of its high consumption of oxygen, its high proportion of polyunsaturated fatty acids, and its exposure to visible light. Although the vision loss of AMD (age-related macular degeneration) results from photoreceptor damage in the central retina, early pathogenesis involves degeneration of retinal pigment epithelial cells.<sup>19</sup> We used ARPE-19 cells (human retinal pigment epithelial cells) to assess the capacity of MitoProbes to detect mitochondrial oxidative stress in a biological milieu. First, we investigated the effect of phorbol 12-myristate 13-acetate (PMA) stimulation in ARPE-19 cells, and its mitigation with MitoProbe I/II. Phorbol esters may be involved with redox-sensitive promoter regions. Upon stimulation with PMA, the cytosolic phox proteins translocate and associate with membrane components and resulting in activation of NADPH oxidase.<sup>19</sup> Initially, superoxide ( $O_2^-$ ) is produced by activated NADPH oxidase. Subsequently,  $O_2^-$  is converted into other reactive oxygen species (ROS), such as  $H_2O_2$ ,  $^{\bullet}OH$ ,  $^1O_2$  and hypochlorous acid (HOCl). Treatment with 0.19  $\mu M$  PMA resulted in a 7–8 fold elevation of ROS levels (Fig. S1), comparable to the ROS increase that occurs in transient ischemia-related disease such as central retinal artery occlusion, angle-closure glaucoma, and carotid artery disease.<sup>19</sup> Furthermore, bright-field transmission measurements following MitoProbe I/II incubation with PMA-treated cells verified that the cells were viable throughout the experiments. These results demonstrate that MitoProbe I/II can passively enter live cells and monitor free radicals generated in the mitochondria (Fig. 2)

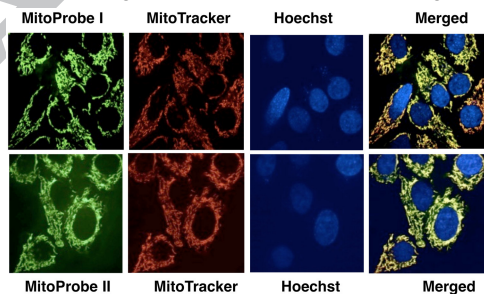


Fig. 2. Confocal laser-scanning fluorescent images of HeLa cells incubated with MitoProbe I (30 nM, green, 45min) or MitoProbe II (50nM, green, 45 min), and stained with MitoTracker (80nM, 45 min, red),

and Hoechst 33242 (0.1  $\mu L/mL$ , 30 min, blue) and overlay images (yellow). Images were obtained with an confocal laser scanning fluorescence microscope using a 40X objective lens in non-FBS, non-phenol red media.

**Mitochondria Undergo Distinct Morphological Changes Under Oxidative Stress.** Changes in mitochondrial morphology serve to adapt the cells to an oxidative environment, and are critical for the survival of retinal and retinal pigment epithelial (RPE) cells because of their high oxygen demand and up-regulated metabolism.<sup>19</sup> The consequences of short-term ROS elevation on cell viability and mitochondrial number has not been extensively investigated. To begin to address this gap in our knowledge, we subsequently investigated the effect of oxidative stress on mitochondrial morphology in human retina pigment epithelial (ARPE) cells. Mitochondrial morphology was visualized with MitoProbes I/II and monitored by confocal fluorescent microscope. We observed that mitochondria undergo distinct morphological changes under conditions of oxidative stress. Following PMA treatment, the morphology of mitochondria in ARPE-19 cells was visualized by MitoProbe application, and could be classified into three categories: tubular (close to normal), intermediate (tubular with swollen regions) and fragmented (small and globular) (Fig. 3).

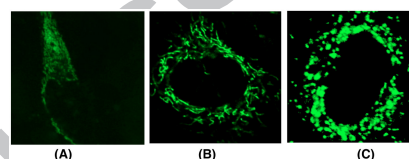
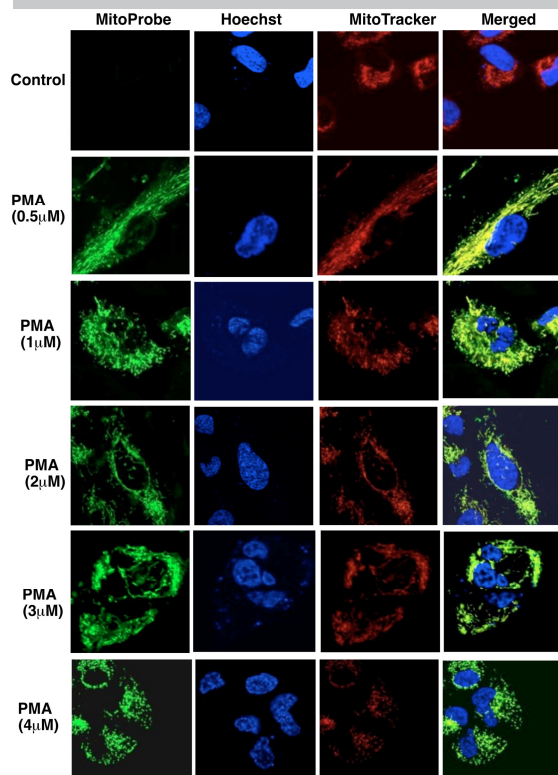


Fig. 3. The mitochondria morphology of ARPE-19 cells visualized by MitoProbes appeared to subdivide into three categories: (A): tubular; (B) intermediate; and (C) fragmented.

In the absence of PMA treatment, ARPE-19 cells exhibited tubular mitochondria and showed weak rhodamine fluorescence upon MitoProbe application. Following treatment with low concentrations of PMA (0.5  $\mu M$ ), a proportion of the cells demonstrated enhanced mitochondrial fluorescence, with MitoProbe I/II being confined to a dispersed network of tubular structures surrounding the nucleus (Fig. 4 and Fig. S2). The mitochondrial location of MitoProbes I/II was confirmed by double labeling with MitoTracker. In contrast to the tubular staining pattern seen in the cells treated with a low-concentration of PMA, a more dispersed and irregular staining pattern, associated with increased mitochondrial fluorescence, was detected in cells treated with higher concentrations of PMA. In addition, considerable amounts of ROS produced by PMA treatment correlated with the fluorescence intensity of MitoProbe I/II.

We next investigated any potential correlations between the concentration of PMA and the potential for, and severity of, mitochondrial fragmentation in ARPE-19 cell lines. We observed a strong correlation between PMA concentration and the percentage of ARPE-19 cells with fragmented mitochondria, as well as a punctiform morphology in the mitochondria showing evidence of fragmentation,



**Fig. 4.** Mitochondria undergo distinct morphological changes under oxidative stress. MitoProbe II (30nM, green, 45 min., column 1) was incubated with ARPE-19 cells and counterstained with Hoechst 33342 (0.1  $\mu\text{L}/\text{mL}$ , 30 min, blue) and Mitotracker (30 nM, red, 45 min). ARPE-19 cells were incubated with varying concentrations of PMA 0.5–4  $\mu\text{M}$ . All images were acquired with an 40 X objective.

Untreated ARPE cells contained primarily long tubular mitochondria, distributed evenly throughout the cell. Increasing the PMA concentration, resulted in mitochondria displaying an intermediate/fragmented mitochondrial structure, suggesting a direct correlation between oxidative stress and fragmentation. Intermediate and fragmented mitochondria accumulated primarily in the perinuclear region of ARPE-19 cells, and these parameters trended upward with increasing concentration of PMA.

**Mitochondria Manifest Partial Recovery After Treatment with Nonlethal Concentrations of PMA.** We next examined the outcomes of non-lethal PMA dosing in ARPE-19 cells as a function of exposure time. PMA treatment (2 hr) followed by culture in PMA-free medium induced significant mitochondrial morphology alterations: transition from the “spaghetti like” pattern indicative of mitochondria of ARPE cells, to vacuolar structures, and eventually to tubular structures once again. Mitochondrial morphology showed signs of recovery after 24h in PMA-free culture medium (Fig. 5 and Fig. S3). This was further suggested by the observation that fragmented mitochondria were present longer than intermediate mitochondria, suggesting that intermediate mitochondria were less damaged and could recover more rapidly.

ARPE-19 cells reverted to tubular mitochondria at 24 hours post PMA-intervention (culture in normal medium), suggesting that a low concentration of PMA only transiently altered the mitochondrial morphology. This reversion could have been the result of fusion of tubular mitochondria, synthesis of new mitochondria, or both. Conversely, ARPE-19 cells treated with higher levels of PMA still manifested significant mitochondrial damage, and recovery was dose-dependent, perhaps indicating that enhanced oxidative damage with higher levels of PMA overwhelmed repair systems. Morphological changes in mitochondria are reminiscent of apoptotic cell death, but generally in response to oxidative stress mitochondria undergo fission, which should be manifest as fragmented mitochondria. The presence of fragmented mitochondria with PMA intervention is suggestive of apoptosis, but not conclusive at this time.

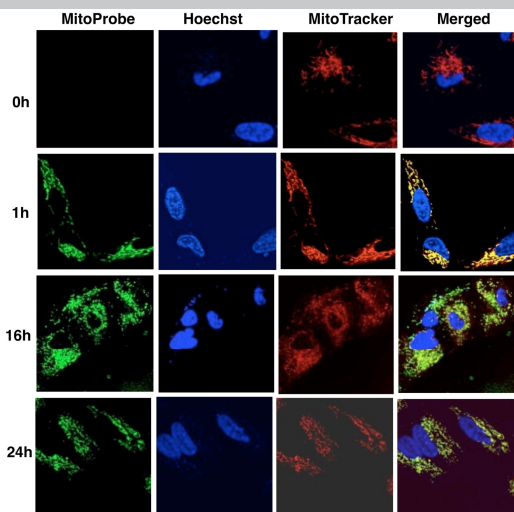


**Fig. 5.** Exposure to a low concentration of PMA induced pronounced, but reversible, morphological changes in the mitochondria of ARPE-19 cells. Representative confocal laser-scanning fluorescence images of ARPE-19 cells incubated with MitoProbe II (30 nM, 45 min., green, column 1) after treatment with 1  $\mu\text{M}$  PMA (except row 1), and co-stained with Hoechst 33342 (0.1  $\mu\text{L}/\text{mL}$ , 30 min, blue) and Mitotracker (30nM, 45 min, red). Cells were imaged after 1, 16 and 24h. All images were acquired with 40 X objective.

Mitochondrial morphology hinges on a balance between mitochondrial fission and fusion, controlled by multiple proteins.<sup>20</sup> We speculate that the oxidative stress induced by non-lethal levels of PMA resulted in unbalanced fusion, and subsequent mitochondrial fragmentation,<sup>20</sup> and that mitochondrial fission/fusion might act as a rescue mechanism for the recovery of damaged mitochondria during PMA intervention.

**MitoProbe I/II is -retained in Fixed, Permeabilized Cells in addition to Actively Dividing Cells.** Previous studies indicated that the fluorescence of rhodamine 123 was almost completely lost upon fixation.<sup>14</sup> We examined this potential effect with MitoProbe I/II and stander acetone/permeabilization in HeLa cells. We observed that the fluorescence intensity of MitoProbe I/II is well-retained for HeLa cells even after fixation with formaldehyde and acetone treatment (Fig. S4 and S5).

**Molecular Dynamic Simulation:** When fluorescent and nitroxide moieties are combined into one molecule, this potentially yields a non- or weakly-fluorescent compound that most likely occurs in relation to the quenching of the excited singlet state of the aromatic fluorescent species by the nitroxide moiety.<sup>16,17</sup> MitoProbe I contains a relatively rigid linker which may be capable of insuring electron exchange between the nitroxide and the fluorophore “through bond” interaction (Fig. 6). MitoProbe II contains a relatively flexible linker that provides the interaction between the nitroxide and fluorophore moieties via “through space” formation of the collision complex. With these distinctions, comparative studies of MitoProbe I and II offered the potential to explore further molecular dynamic considerations in our probes.

In a biological environment, nitroxides undergo one electron reduction and oxidation, a key feature of their free radical scavenging capability. The free radical scavenging effect of nitroxide derivatives is correlated with selected molecular and biochemical parameters such as the highest occupied molecular orbital (HOMO) energy, the net charge, and the difference in the heat of formation between hydroxylamine and its radical.<sup>21,22,24</sup>

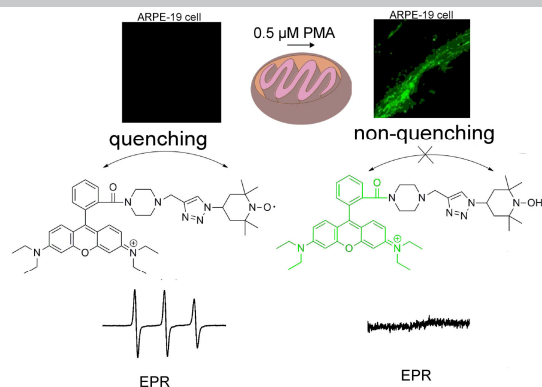


Fig. 6. Proposed acting mechanism of MitoProbe.

The ionization energy of the HOMO can be exploited as a measure of a free radical scavenger's capacity to participate in radical scavenging reactions. For example, the HOMO energy of melatonin (a natural antioxidant) is  $-10.425$  eV. In comparison, the HOMO energy of our MitoProbes is:  $E_{\text{HOMO}}$  (MitoProbe I) =  $-4.983$  eV and  $E_{\text{HOMO}}$  (MitoProbe II) =  $-5.224$  eV. The higher the HOMO energy, the more active the compound would be expected to demonstrate as a free radical scavenger. Theoretically, MitoProbes should possess much higher radical trapping potential than a compound such as melatonin. MitoProbe I is generally predicted to be a slightly more active free radical scavenger than MitoProbe II. However, there were no statistically significant differences between these two fluorescent probes in our present study with respect to their capacity to scavenge radicals. It will be of interest to quantitatively compare the chemical analyses of MitoProbes I/II in frozen tissue samples, and to correlate those findings with our redox imaging results. Such a correlation will serve to establish a novel calibration procedure for gauging the true concentrations of the endogenous MitoProbe I /II. These studies are in progress.

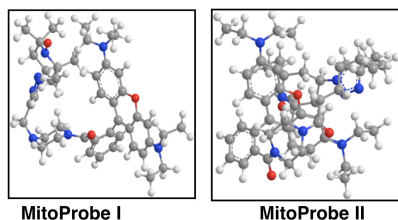


Fig. 7. Predicted lowest energy conformations of MitoProbes I/II.

In conclusion, the development of MitoProbes that specifically accumulate within mitochondria coupled to the capacity to monitor mitochondrial oxidative stress via real-time imaging microscopy, will greatly improve our understanding of mitochondrial function, morphology and dynamics. These tools, and their further development, will lead to a more comprehensive understanding of the molecular basis of mitochondrial dynamics and its impairment in different diseases, leading to more targeted therapeutic strategies. The continued success of our work will also extend a pathway to imaging of mitochondrial oxidative stress in cryogenic biopsy specimens, adding an additional tool to diagnosis of oxidative stress-mediated diseases, even in the post-mortem state.

**Acknowledgment.** L.B. is grateful to NIH (GM088795-01), NSF (No. 1048655), NASA (# MSGC R85197), MIIE (#1204010), VPR-SI fund (#R01386), and the Research Excellence Fund (#R01121 and #R01323).

The authors are particularly thankful to Dr. Bruce Seely for his ongoing support of our work.

## REFERENCE

- (1.) Bowerman, B. *Science* **2005**, 308, 1119.
- (2.) Cho, D. H.; Nakamura, T.; Fang, J. G.; Cieplak, P.; Godzik, A.; Gu, Z.; Lipton, S. A. *Science* **2009**, 324, 102.
- (3.) Coyle, J. T.; Puttfarcken, P. *Science* **1993**, 262, 689.
- (4.) Dawson, T. M.; Dawson, V. L. *Science* **2003**, 302, 819.
- (5.) Green, D. R.; Galluzzi, L.; Kroemer, G. *Science* **2011**, 333, 1109.
- (6.) Green, D. R.; Reed, J. C. *Science* **1998**, 281, 1309.
- (7.) Kujoth, G. C.; Hiona, A.; Pugh, T. D.; Someya, S.; Panzer, K.; Wohlgemuth, S. E.; Hofer, T.; Seo, A. Y.; Sullivan, R.; Jobling, W. A.; Morrow, J. D.; Van Remmen, H.; Sedyvy, J. M.; Yamasoba, T.; Tanokura, M.; Weindruch, R.; Leeuwenburgh, C.; Prolla, T. A. *Science* **2005**, 309, 481.
- (8.) Lustbader, J. W.; Cirilli, M.; Lin, C.; Xu, H. W.; Takuma, K.; Wang, N.; Caspersen, C.; Chen, X.; Pollak, S.; Chaney, M.; Trinchese, F.; Liu, S. M.; Gunn-Moore, F.; Lue, L. F.; Walker, D. G.; Kuppasamy, P.; Zewier, Z. L.; Arancio, O.; Stern, D.; Yan, S. S. D.; Wu, H. *Science* **2004**, 304, 448.
- (9.) Miller, R. A. *Science* **2005**, 308, 1875-1876.
- (10.) Rabinowitz, J. D.; White, E., *Autophagy and Metabolism*. *Science* **2010**, 330, 1344-1348.
- (11.) Wallace, D. C. *Science* **1999**, 283, 1482-1488.
- (12.) Koide, Y.; Urano, Y.; Kenmoku, S.; Kojima, H.; Nagano, T. *J. Am. Chem. Soc.* **2007**, 129, 10324.
- (13.) Robinson, K. M.; Janes, M. S.; Pehar, M.; Monette, J. S.; Ross, M. F.; Hagen, T. M.; Murphy, M. P.; Beckman, J. S. *Proc. Natl. Acad. Sci. U S A* **2006**, 103, 15038.
- (14.) *Methods in Cell Biology: Fluorescent Labelling*; Chen, L. B.; Academic Press Limited: San Diego, California, **1989**, 29, 103.
- (15.) Dickinson, B. C.; Huynh, C.; Chang, C. J. *J. Am. Chem. Soc.* **2010**, 132, 5906.
- (16.) Green, S. A.; Simpson, D. J.; Zhou, G.; Ho, P. S.; Blough, N. V. *J. Am. Chem. Soc.* **1990**, 112, 7337.
- (17.) Yapici, N. B.; Jockusch, S.; Moscatelli, A.; Mandalapu, S. R.; Itagaki, Y.; Bates, D. K.; Wiseman, S.; Gibson, K. M.; Turro, N. J.; Bi, L. R. *Org. Lett.* **2012**, 14, 50.
- (18.) Le Droumaguet, C.; Wang, C.; Wang, Q. *Chem. Soc. Rev.* **2010**, 39, 1233.
- (19.) Schrier, S. A.; Falk, M. J. *Curr. Opin. Ophthalmol.* **2011**, 22, 325.
- (20.) Youle, R. J.; van der Bliek, A. M. *Science* **2012**, 337, 1062-1065.
- (21.) Bi, W.; Li, X. X.; Bi, Y.; Xue, P.; Zhang, Y.; Gao, X.; Wang, Z.; Li, M.; Itagaki, Y.; Bi, L. *J. Med. Chem.* **2012**, 55, 4501.
- (22.) Bi, W.; Bi, Y.; Xue, P.; Zhang, Y.; Gao, X.; Wang, Z.; Li, M.; Baudy-Floc'h, M.; Ngerebara, N.; Gibson, K. M.; Bi, L. *J. Med. Chem.* **2010**, 53, 6763.
- (23.) *Progress in Molecular Biology and Translational Science: Biology of mitochondria in neurodegenerative diseases*; Martin, L. J. Academic Press, Elsevier: San Diego, USA, **2012**; Vol. 107, 355.
- (24.) Pajca, A.; Mukherjee, S.; Pink, M.; Rajca, S. *J. Am. Chem. Soc.* **2006**, 128, 13497-13507.
- (25.) Gurney, M.E.; Pu, H.; Chiu, A.Y.; Dal Canto, M.C.; Polchow, C.Y.; Alexander, D.D.; Caliendo, J.; Hentati, A.; Kwon, Y.W.; Deng, H.X.; Chen, W.; Zhai, P.; Sufit, R.L.; Siddique, T. *Science*, **1994**, 264, 1772.
- (26.) Dickinson, B. C.; Lin, V. S.; Chang, C. J. *Nat. Protoc.* **2013**, 8, 1249-1259

